Near IR luminescent rare earth 3,4,5,6-tetrafluoro-2-nitrophenoxide complexes: Synthesis, X-ray crystallography and spectroscopy

Zheng, YX; Motevalli, M; Tan, RHC; Abrahams, I; Gillin, WP; Wyatt, PB

For additional information about this publication click this link.
http://qmro.qmul.ac.uk/jspui/handle/123456789/1162

Near IR Luminescent Rare Earth 3,4,5,6-Tetrafluoro-2-nitrophenoxide Complexes: Synthesis, X-ray Crystallography and Spectroscopy (manuscript published as doi:10.1016/j.poly.2008.01.022)

Youxuan Zheng,[†‡] Majid Motevalli,[†] Rendy H. C. Tan,[†‡] Isaac Abrahams,[†] William P. Gillin[‡] and Peter B. Wyatt*[†]

School of Biological and Chemical Sciences and Department of Physics, Queen Mary, University of London, Mile End Road, London, UK E1 4NS

[†] School of Biological and Chemical Sciences

[‡] Department of Physics

*Corresponding author. Tel.: +44 (20) 7882 3267; Fax: +44 (20) 7882 7427.

E-mail address: p.b.wyatt@qmul.ac.uk (P. B. Wyatt).

Abstract

3,4,5,6-Tetrafluoro-2-nitrophenoxide (L^-) forms complexes with rare earth M^{3+} ions. X-ray crystal structures of substances with the stoichiometry $Cs_2ML_5 \cdot mEt_2O$ (M = Er, $m = 0$; M = Er, $m = 1$; M = Y, $m = 1.5$; M = Yb, $m = 1$) have been determined. Each M^{3+} ion is coordinated to two bidentate and three monodentate L^- ions; Et_2O does not coordinate to M^{3+}. The complexes absorb both visible and ultraviolet light. The solid Er^{3+} and Yb^{3+} complexes have unusually long lifetimes (τ = 20.2 μs and 142 μs respectively) for the decay of their luminescence in the near infrared region following photoexcitation; this is attributed to the lack of C–H bonds and other high frequency oscillators that could cause vibrational quenching.

1. Introduction

Most lanthanide ions are luminescent: their ability to emit at well-defined wavelengths, even in the condensed phases, makes them particularly suitable for use in applications such as sensors, light sources and display devices. Near-infrared radiation is transmitted through biological tissue and optical fibres with little absorption. Ions such as Er^{3+}, Yb^{3+} and Nd^{3+}, that emit in this region, are of therefore of particular interest [1]. The forbidden nature of f-f transitions means that the cross sections for direct photoexcitation of lanthanide ions are low, so that although optical amplifiers containing erbium-doped glasses are used widely in modern telecommunications, these devices are bulky and expensive. Several research groups have examined the synthesis and properties of organic complexes containing additional chromophores to act as antennae and effect the photoexcitation of the lanthanide ions. Examples include conjugated and aromatic organic systems [2], transition metal complexes [3] and those containing a second lanthanide ion with a larger extinction coefficent [4].

Organic ligands and coordinated solvent molecules usually contain C–H and O–H bonds that cause rapid vibrational quenching of luminescence in the infrared region [5]. Deuteration of hydrogen-containing ligands, together with exclusion of coordinated water, can extend the lifetime of infrared luminescence from lanthanide complexes [6]. However, full deuteration of ligands is rarely achieved and the presence of any ^1H within 20 Å of an Er^{3+} ion can be lifetime-limiting [7]. The use of fluorinated ligands such as $(C_8F_{17}SO_2)_2N^-$ and $[(C_6F_5)_2PO]_2N^-$ is another option [8,9]. The Er^{3+} salt of the latter ligand shows remarkably long luminescence lifetimes of up to 0.74 ms, although this remains at least an order of magnitude less than the natural radiative lifetime of the ion [10]. Highly fluorinated ligands may confer other useful properties on their metal complexes, such as oxidative resistance and fluorocarbon solubility [11], whilst the special characteristics of materials containing perfluoroaryl groups are being exploited in organic semiconductors [12]. It has been predicted that Er^{3+} complexes of fully halogenated ligands may eventually show emission quantum yields close to 100% [13]. An additional requirement for efficient photosensitization of Er^{3+} is the ability to absorb visible light. Since the existing fully halogenated ligands do not possess this feature, we are now investigating new ligand systems that combine the absence of hydrogen atoms with the provision of a chromophore.

Potassium 2-nitrophenoxide is known to combine with lanthanide ions to give a range of chains, layers and clusters [14]. We now report the synthesis, structures and luminescence properties for the first metal complexes to be prepared using the orange-coloured salts of 3,4,5,6-tetrafluoro-2-nitrophenol (**1**), a compound which is easily made by hydrolysis of commercially available pentafluoronitrobenzene, following the literature procedure [15]. We show that it is able to exclude hydrogen from the environs of lanthanide ions as well as absorbing visible light. We chose to introduce this ligand as its caesium salt, in the hope of preparing analogues of the volatile, anhydrous salts such as $Cs[Er(HFA)_4]$, where HFA = 1,1,1,5,5,5-hexafluoroacetylacetonate. However, even when the caesium salt of **1** was mixed with erbium chloride in a 4:1 molar ratio, a crystalline complex with the stoichiometry Cs_2ErL_5 (L = tetrafluoro-2-nitrophenoxide) was isolated. Our investigations have therefore focused on complexes of this type.

2. Experimental

2.1 Instrumentation and General procedures. ^{19}F NMR spectra were obtained on a Bruker AMX400 and the chemical shifts were referenced to external CFCl$_3$. MALDI mass spectra were recorded using a Bruker Daltonics Autoflex. CI mass spectra were obtained by the EPSRC National Mass Spectrometry Service Centre, Swansea using a Finnigan MAT 95XP. CHN elemental analyses were performed by MEDAC Ltd, Egham, Surrey. All photoluminescence experiments were conducted using solid samples of the metal complexes. Excitation was by ~7 ns pulses from a Continuum Panther optical parametric oscillator (OPO) pumped with a Surelite I laser. The luminescence was dispersed in a Triax 550 spectrometer and detected using a Hamamatsu R5509-72 infrared photomultiplier tube.

2.2 X-ray crystallography. Data for **2**, **3** and **7** were collected at 120 K using a Nonius Kappa CCD area detector diffractometer mounted at the window of molybdenum rotating anode (50 kV, 90 mA, λ = 0.71069 Å). The crystal-to-detector distance was 30 mm and ϕ and ω scans were carried out to fill the Ewald sphere. Data collection and processing were carried out using COLLECT [16], DENZO [17] and maXus [18] and empirical absorption correction was applied using SORTAV [19]. Data for **5** were collected on a CAD-4 diffractometer using λ = 0.71069 Å with ω-2θ scans at 160 K. The unit cell parameters were determined by least-squares refinement on diffractometer angles for 25 automatically centred reflections [20]. Data for **5** were corrected for absorption by empirical methods (ψ scan) [21] and for Lorentz-polarization effects by XCAD4 [22].

The structures were solved by heavy-atom methods using SHELXS-97 and DIRDIF-99 programs [23, 24], and were refined anisotropically (non-hydrogen atoms) by full-matrix least-squares on F^2 using SHELXL-97. The H atoms were calculated geometrically and refined using the riding model facility in the SHELXL-97 programme. Solvent molecules were located in the crystal structures of **3**, **5** and **7**. All showed relatively high anisotropic thermal parameters, reflecting not only a high degree of thermal motion, but also a degree of positional disorder. In the case of **5**, two unique solvent molecules were located in the asymmetric unit. One was found to be fully occupied, however the second which lies close to the two-fold axis was fixed at half occupancy as indicated by a refinement of the fractional site occupancies for the atoms in this molecule. Interatomic distances in the solvent molecules in the structure of **5** were restrained to lie within the accepted ranges. The programs ORTEP-3 [25] and PLATON [26] were used for diagrams and WINGX [27] was used to prepare material for publication.

2.3 Synthesis

Cs$_2$Er(o-O$_2$N-C$_6$F$_4$-O)$_5$ (2)

o-O$_2$N-C$_6$F$_4$-OH (0.422 g, 2.0 mmol) and Cs$_2$CO$_3$ (0.326 g, 1.0 mmol) were dissolved in a mixture of MeCN (10 mL) and H$_2$O (3 mL) with stirring at room temperature. A solution of ErCl$_3$·6H$_2$O (0.153 g, 0.40 mmol) in water (3 mL) was

then added dropwise. After 2 h the solvent was evaporated to dryness under reduced pressure and the residue was extracted with Et_2O (3 × 10 mL). The Et_2O extract was filtered, concentrated and the residue recrystallized from Et_2O-hexane to give $Cs_2Er(o\text{-}O_2N\text{-}C_6F_4\text{-}O)_5$ (**2**) (0.338 g, 57%) as orange blocks. Found: C, 24.55; H, 0.10; N, 5.01. Calcd for $C_{30}Cs_2ErF_{20}N_5O_{15}$: C, 24.29; H, 0.00; N, 4.72; λ_{max}/nm (MeCN) 223 (ε = 64000), 266 (17700), 406 (11000); ν_{max}/cm^{-1} (KBr) 1659 (C=C), 1541 (NO_2), 1512 (NO_2); δ_F (377 MHz, DMSO-d_6) –180 (br), –157 (br), –153.9, –149.9, m/z (CI–) Found: 1144 (14%), 1143 (48), 1142 (24), 1141 (100), 1140 (91), 1139 (94), 1138 (1), 1137 (5). Calculated for $C_{24}CsErF_{16}N_4O_{16}$ (M–$O_2N\text{-}C_6F_4\text{-}OCs$): 1144 (11), 1143 (44), 1142 (14), 1141 (79), 1140 (68), 1139 (100), 1138 (1), 1137 (5).

$Cs_2(Et_2O)Er(o\text{-}O_2N\text{-}C_6F_4\text{-}O)_5$ (3)

This was prepared as for **2** and obtained as yellow blades following recrystallisation from Et_2O-pentane or Et_2O-CCl_4 by layering of solvents at room temperature. Found: C, 26.60; H, 0.52; N, 4.27. Calcd for $C_{34}H_{10}Cs_2ErF_{20}N_5O_{15}$: C, 26.22; H, 0.65; N, 4.50. λ_{max}/nm (MeCN) 222 (ε = 67000), 267 (20800), 421 (16100); ν_{max}/cm^{-1} (KBr) 2982 (C–H), 2883 (C–H), 1655 (C=C), 1541 (NO_2), 1508 (NO_2).

$Cs_2Y(o\text{-}O_2N\text{-}C_6F_4\text{-}O)_5$ (4)

This was prepared by analogy with the Er complex **2** and was obtained in 70% yield as orange prisms. Found: C, 26.00; H, <0.10; N, 5.11. Calcd for $C_{30}Cs_2F_{20}N_5O_{15}Y$: C, 25.65; H, 0.00; N, 4.98; λ_{max}/nm (MeCN) 227 (ε = 58000), 267 (18200), 403 (12000); ν_{max}/cm^{-1} (KBr) 1653 (C=C), 1541 (NO_2), 1506 (NO_2); δ_F (377 MHz, DMSO-d_6) –184 (br), –160.0, –155.4, –150.9; on heating the NMR solution to 60 °C an irreversible change occurred which caused the peaks to become sharper and to shift to the following positions –173.7 (m), –157.0 (d, J = 23 Hz), 151.5 (t, J = 23 Hz), 149.0 (dd, J = 26, 4 Hz); m/z (MALDI–) 929 {[Y($o\text{-}O_2N\text{-}C_6F_4\text{-}O)_4$]$^-$, 100%}, 738 {[Y($o\text{-}O_2N\text{-}C_6F_4\text{-}O)_3$F]$^-$, 3%}, 210 {($o\text{-}O_2N\text{-}C_6F_4\text{-}O)^-$, 51%}; m/z (CI–) Found: 1063.5 (6%), 1062.4 (26), 1061.4 (100). Calculated for $C_{24}CsF_{16}N_4O_{16}Y$ (M–$o\text{-}O_2N\text{-}C_6F_4\text{-}OCs$): 1063.7 (4), 1062.7 (26), 1061.7 (100).

$Cs_2(Et_2O)_{1.5}Y(o\text{-}O_2N\text{-}C_6F_4\text{-}O)_5$ (5)

By analogy with the preparation of **3**, recrystallisation by layering ether with hexane at room temperature gave crystals of the sesqui-etherate **5** as orange blocks that were suitable for X-ray analysis, but which readily lost solvent.
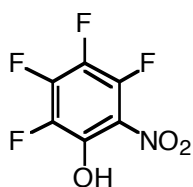
$Cs_2(Et_2O)_{0.5}Yb(o\text{-}O_2N\text{-}C_6F_4\text{-}O)_5$ (6)

This was prepared by analogy with the Er complex **2** and was obtained in 66% yield as orange prisms. Found: C, 25.16; H, 0.15; N, 4.78. Calcd for $C_{30}Cs_2F_{20}N_5O_{15}Yb\cdot0.5Et_2O$: C, 25.18; H, 0.33; N, 4.59; λ_{max}/nm (MeCN) 223

(ε = 50000), 266 (17100), 403 (10400) ν_{max}/cm^{-1} (KBr) 2940 (C-H), 1659 (C=C), 1541 (NO$_2$) and 1512 (NO$_2$); δ_F (377 MHz, DMSO-d_6) –185 (br), –164 (br), –157.6, –153.0; m/z (MALDI–) 1014 {[^{174}Yb(o-O$_2$N-C$_6$F$_4$-O)$_4$]$^-$, 87%}, 823 {[^{174}Yb(o-O$_2$N-C$_6$F$_4$-O)$_3$F]$^-$, 10%}, 210 {(o-O$_2$N-C$_6$F$_4$-O)$^-$, 100%}; m/z (CI–) Found: 1150 (8%), 1149 (42), 1148 (29), 1147 (100), 1146 (59), 1145 (67), 1144 (32). Calculated for C$_{24}$CsF$_{16}$N$_4$O$_{16}$Yb (M$^-$ – o-O$_2$N-C$_6$F$_4$-OCs): 1150 (10), 1149 (40), 1148 (26), 1147 (100), 1146 (50), 1145 (69), 1144 (44).

Cs$_2$(Et$_2$O)$_{0.5}$Yb(o-O$_2$N-C$_6$F$_4$-O)$_5$ (7)

By analogy with the preparation of **3**, recrystallisation by layering ether with hexane at room temperature gave crystals of **7** as orange blocks that were suitable for X-ray analysis.

1

Scheme 1. Chemical structure of 3,4,5,6-tetrafluoro-2-nitrophenol.

Table 1. Crystallographic details and metal-ligand bond lengths of $Cs_2Er(o\text{-}O_2N\text{-}C_6F_4\text{-}O)_5$ (**2**), $Cs_2(Et_2O)Er(o\text{-}O_2N\text{-}C_6F_4\text{-}O)_5$ (**3**), $Cs_2(Et_2O)_{1.5}Y(o\text{-}O_2N\text{-}C_6F_4\text{-}O)_5$ (**5**) and $Cs_2(Et_2O)Yb(o\text{-}O_2N\text{-}C_6F_4\text{-}O)_5$ (**7**).

	2	3	5	7
Formula	$C_{30}Cs_2ErF_{20}N_5O_{15}$	$C_{34}H_{10}Cs_2ErF_{20}N_5O_{16}$	$C_{36}H_{15}Cs_2F_{20}N_5O_{16.5}Y$	$C_{34}H_{10}Cs_2F_{20}N_5O_{16}Yb$
Formula weight	1483.43	1557.55	1516.26	1563.33
Temperature	120(2) K	120(2) K	160(2) K	120(2) K
Crystal system	Triclinic	Monoclinic	Monoclinic	Monoclinic
Space group	P-1	$P2_1/c$	$I2/a$	$P2_1/c$
a	8.5213(2) Å	13.1114(3) Å	23.630(9) Å	13.0900(3) Å
b	13.9433(5) Å	23.3692(5) Å	15.129(2) Å	23.3001(6) Å
c	17.5709(7) Å	15.0055(2) Å	28.778(7) Å	15.0004(3) Å
α	91.266(2)°	90°	90°	90°
β	103.680(2)°	96.1220(10)°	99.09(2)°	96.1676(13)°
γ	102.206(2)°	90°	90°	90°
V	1976.89(12) Å³	4571.51(16) Å³	10159(5) Å³	4548.61(18) Å³
Z	2	4	8	4
Density (calculated)	2.492 Mg/m³	2.263 Mg/m³	1.983 Mg/m³	2.283 Mg/m³
Absorption coefficient	4.110 mm⁻¹	3.562 mm⁻¹	2.705 mm⁻¹	3.791 mm⁻¹
Reflections collected	39686	54306	19158	45269
Independent reflections	9020 [R_{int} = 0.0440]	10416 [R_{int} = 0.0556]	9424 [R_{int} = 0.1223]	10328 [R_{int} = 0.0354]
Final R indices [$I > 2\sigma(I)$]	$R1 = 0.0334$, $wR2 = 0.0725$	$R1 = 0.0340$ $wR2 = 0.0660$	$R1 = 0.0586$, $wR2 = 0.1126$	$R1 = 0.0264$, $wR2 = 0.0644$
R Indices (all data)	$R1 = 0.0516$, $wR2 = 0.0795$	$R1 = 0.0499$ $wR2 = 0.0715$	$R1 = 0.1812$, $wR2 = 0.1451$	$R1 = 0.0307$, $wR2 = 0.0669$

Table 2. Metal-ligand distances/Å for $Cs_2Er(o\text{-}O_2N\text{-}C_6F_4\text{-}O)_5$ (**2**), $Cs_2(Et_2O)Er(o\text{-}O_2N\text{-}C_6F_4\text{-}O)_5$ (**3**), $Cs_2(Et_2O)_{1.5}Y(o\text{-}O_2N\text{-}C_6F_4\text{-}O)_5$ (**5**) and $Cs_2(Et_2O)Yb(o\text{-}O_2N\text{-}C_6F_4\text{-}O)_5$ (**7**).

	2	3	5	7
M–O (mondentate phenoxide)	2.186(3)	2.181(3)	2.193(6)	2.150(2)
	2.220(3)	2.235(3)	2.221(6)	2.208(2)
	2.251(3)	2.255(3)	2.249(6)	2.224(2)
M–O (bidentate phenoxide)	2.231(3)	2.220(3)	2.224(6)	2.197(2)
	2.239(3)	2.236(3)	2.232(6)	2.213(2)
M–O (nitro group)	2.370(3)	2.461(3)	2.439(7)	2.438(2)
	2.525(3)	2.464(3)	2.473(7)	2.459(2)

Table 3. Bond angles at erbium for $Cs_2Er(o\text{-}O_2N\text{-}C_6F_4\text{-}O)_5$ (**2**).

| Angles/° at Er	O(1)	O(4)	O(7)	O(9)	O(10)	O(13)
O(4)	85.77(11)					
O(7)	86.14(11)	145.95(11)				
O(9)	74.56(11)	76.87(10)	69.10(10)			
O(10)	151.16(12)	86.18(11)	85.19(12)	76.66(11)		
O(13)	122.58(11)	127.12(11)	84.50(11)	148.12(10)	83.84(11)	
O(15)	76.16(12)	76.21(11)	133.15(12)	141.26(10)	128.25(12)	70.31(10)

3. Results and discussion

3.1 Crystal growth and X-ray crystallography. The rare earth complexes were prepared in aqueous acetonitrile, which was then evaporated and the residue was extracted with boiling diethyl ether. Concentration of the ether extracts and the addition of pentane, hexane or carbon tetrachloride led to the formation of crystals. Samples used for X-ray diffraction were obtained by layering of solvents at room temperature and were dried only briefly, since prolonged drying under vacuum caused some of the crystals to lose their transparency. Two crystalline erbium complexes were characterized: orange blocks **2** (stoichiometry Cs_2ErL_5) and yellow blades **3** (an etherate, $Cs_2ErL_5 \cdot Et_2O$). Formation of the unsolvated product **2** was favoured when solvent was allowed to evaporate from a boiling solution of the complex in Et_2O-hexane, whereas the etherate **3** crystallized following slow diffusion of CCl_4 or pentane into an ethereal solution of the complex

at *ca* 18 °C. Ether of crystallization was also present in the other two complexes that were used for X-ray diffraction [Cs$_2$YL$_5$·1.5Et$_2$O (**5**) and Cs$_2$YbL$_5$·Et$_2$O (**7**)].

The structure of the unsolvated erbium complex **2** is shown in Figure 1; crystallographic details, metal-ligand bond lengths and selected bond angles are provided in Tables 1-3. In the crystal structure of Cs$_2$YL$_5$·1.5Et$_2$O (**5**) the space group *I2/a* was used as a non-standard setting of *C2/c* in order to give a smaller *β* angle. The coordination of the tetrafluoronitrophenoxide ligands to the rare earth ions in the four crystal structures is very similar. Each M^{3+} ion is bound to five aryloxide ligands, of which three are monodentate; the remaining two ligands are additionally coordinated to the rare earth through one oxygen atom of the nitro group, making them bidentate and giving a coordination number of seven. Similar coordination about the rare earth has been reported for K$_2$Ln(*o*-O$_2$NC$_6$H$_4$O)$_5$ (Ln = Sm, Eu) [14], but the structures of these two potassium salts incorporate pentane of crystallization within the distinct channels that are present. The possibility that 2-nitrophenoxide units can be both monodentate and bidentate has also been established in the chemistry of lanthanide picrates [28]. The Et$_2$O molecules in our solvated complexes are somewhat disordered, particularly so in the case of the yttrium derivative **5**, but it is clear that none of this solvent coordinates to the rare earth metals. The geometry about the rare earth ions in complexes **2**, **3**, **5** and **7** is irregular. The bidentate nitrophenoxide ligands have narrow O–M–O bite angles, in the range 68-72°. The M ions are significantly closer to the phenoxide oxygen atoms than to the oxygen atoms of the coordinating nitro groups; for example the Er–O contacts range between 2.18-2.24 Å (phenoxide) and 2.37-2.53 Å (NO$_2$).
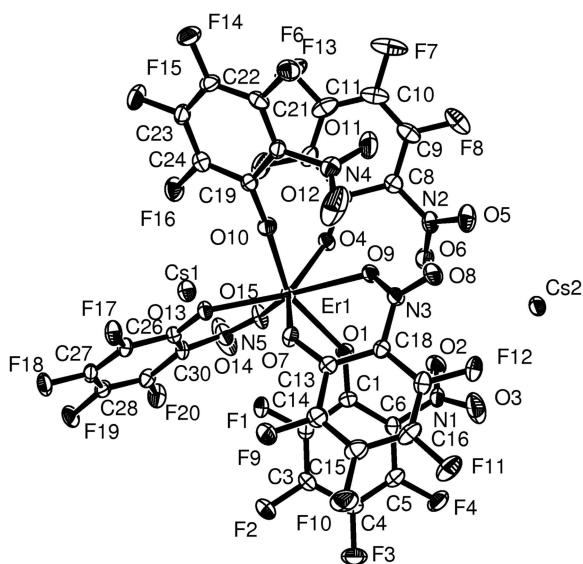
Figure 1. Solid state structure of Cs$_2$Er(*o*-O$_2$N-C$_6$F$_4$-O)$_5$ (**2**) showing the coordination of Er.

The two crystallographically distinct Cs$^+$ ions in the solvent-free form of **2** make contacts with the phenoxide and nitro groups, so that each caesium atom has eight oxygen atoms within 3.4 Å. In addition some close Cs–F contacts are

present, so that Cs (1) is only 3.13 Å from F(17), which is thus its closest neighbour, and 3.34 Å from F(19). Plenio has noted that the distribution of CF...Cs$^+$ contacts in the literature shows a clear maximum in the range 3.2-3.4 Å, providing evidence for an attractive Cs–F interaction [29]. The structures of the etherates again show contact of Cs$^+$ with both fluorine and oxygen atoms, including those of Et$_2$O.

3.2 Spectroscopic and analytical characterization. Analytical samples were dried for several days at *ca* 20 °C and 1 mmHg, after which CHN combustion analysis indicated that materials with the compositions Cs$_2$ErL$_5$ (**2**), Cs$_2$ErL$_5$·Et$_2$O (**3**), Cs$_2$YL$_5$ (**4**) and Cs$_2$YbL$_5$·0.5Et$_2$O (**6**) had been obtained. Weak IR absorptions close to 2970 cm^{-1} and small amounts of hydrogen found by combustion analysis indicate that some solvent is present at low levels (<20 mol%) in bulk samples of the 'unsolvated' materials. Removal of the remaining Et$_2$O from Cs$_2$YbL$_5$·0.5Et$_2$O (**6**) was attempted by heating under reduced pressure; significant loss in mass occurred only on heating above 120 °C and under these conditions the darkening of the sample indicated decomposition. Attempts to sublime the complexes *in vacuo* also led to decomposition.

Compounds **2**, **4** and **6** were further characterized by ^{19}F NMR, IR, UV and mass spectrometry. Despite the considerable peak broadening in the ^{19}F NMR spectra (376 MHz, DMSO-d_6, T = 27 °C) of the paramagnetic Er^{3+} and Yb^{3+} derivatives **2** and **6**, four fluorine environments were clearly resolved in each case. The ^{19}F NMR spectrum of the Y^{3+} salt **4** also showed some broadening, particularly in the case of the most upfield peak (assigned as F-6). This suggested that the complex might be fluxional and the spectrum was therefore recorded at a higher temperature (60 °C). The peaks became much sharper, but they then remained sharp after cooling the sample back to 27 °C, which is consistent with an irreversible ligand displacement by DMSO. Mass spectra in chemical ionization mode showed strong [CsML$_4$]$^-$ negative ions with the expected isotopic distribution patterns. UV-visible spectra were recorded in acetonitrile solution and all the compounds showed similar spectra, which were dominated by three strong absorption bands of the ligand. The longest wavelength absorptions occurred at λ_{max} between 402-406 nm in acetonitrile solutions of concentrations of *ca* 10^{-4} M. Fivefold dilution with acetonitrile caused the λ_{max} of the longest wavelength band to increase to 415-428 nm; this shift was accompanied by an increase in the ε value and again suggests the occurrence of solvolysis.

3.3 Photoluminescence studies. Figure 2 shows the photoluminescence spectra for the Cs$_2$(Et$_2$O)$_{0.5}$Yb(*o*-O$_2$N-C$_6$F$_4$-O)$_5$ (**6**) and Cs$_2$Er(*o*-O$_2$N-C$_6$F$_4$-O)$_5$ (**2**) samples. Both materials show luminescence characteristic of the central ion with emission for the ^{2}F$_{5/2}$ → ^{2}F$_{7/2}$ transition for ytterbium and for the ^{4}I$_{13/2}$ → ^{4}I$_{15/2}$ transition for the erbium ion. For ytterbium an excitation wavelength of 460 nm was used. In the case of erbium an excitation wavelength of 520 nm was chosen to provide direct excitation into the ^{2}H$_{11/2}$ level of the Er^{3+} ion, which rapidly decays to the ^{4}I$_{13/2}$ level. The shapes of the photoluminescence spectra for both materials are independent of excitation wavelength. The rise time of the ^{4}I$_{13/2}$ → ^{4}I$_{15/2}$

transition gives a direct measurement of the decay time from the initially excited state into the $^4I_{13/2}$ level and was measured to be of the order of 25 ns. Photoluminescence excitation (PLE) spectroscopy of both samples (Figure 3) was recorded by monitoring the output from the peak of the ion-related photoluminescence whilst changing the excitation wavelength over the range 410 nm to 680 nm. For the ytterbium complex **6** the PLE spectrum shows a broad feature peaking at ~520 nm and a second feature extending to shorter wavelengths (< 410 nm). Also shown in Figure 3 is the absorption spectrum of this complex which is a broad band with a peak at ~400 nm. This feature in the absorption spectra can be assumed to be the absorption into the singlet state of the ligand. The majority of the absorption that results in ytterbium emission therefore appears to come from another band at longer wavelengths than the singlet absorption. We suggest that this may be direct absorption into the triplet state, the long lifetime of which encourages transfer into the ytterbium ion. This absorption is weak, so is not seen in the visible absorption spectrum where it is masked by the tail of the singlet absorption. Also shown in Figure 3 is the PLE spectrum of $Cs_2Er(o\text{-}O_2N\text{-}C_6F_4\text{-}O)_5$ **2**. This has the same shape as that for $Cs_2Yb(Et_2O)_{0.5}(o\text{-}O_2N\text{-}C_6F_4\text{-}O)_5$ **6** but with additional peaks due to direct absorption into the Er^{3+} ions. To illustrate this the absorption spectrum of a solution of erbium chloride in methanol is also given which shows the narrow absorption into erbium ions. The fact that these lines are superimposed upon the same broad feature that was observed for the $Cs_2Yb(Et_2O)_{0.5}(o\text{-}O_2N\text{-}C_6F_4\text{-}O)_5$ **6** shows that the ligand is acting as a weak sensitizer for erbium as well as for ytterbium. The rise time for the $^4I_{13/2} \rightarrow {}^4I_{15/2}$ transition was found to be independent of the excitation wavelength used. This suggests that energy transfer from the ligand to the erbium ion is not the rate-limiting step in the energy migration. For the $Cs_2Yb(Et_2O)_{0.5}(o\text{-}O_2N\text{-}C_6F_4\text{-}O)_5$ **6** the rise time was found to be identical to the laser response (~7 ns) which supports this observation.
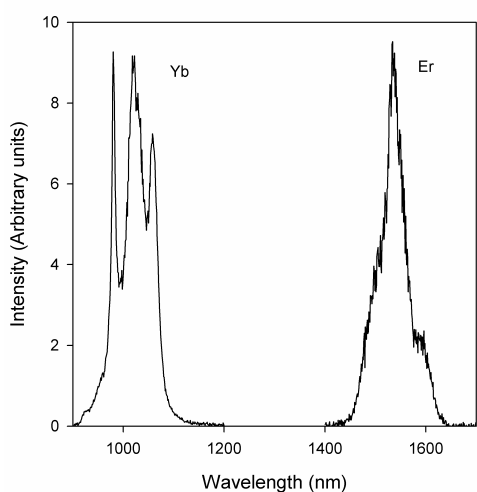
Figure 2. Near infrared photoluminescence spectra for $Cs_2Yb(Et_2O)_{0.5}(o\text{-}O_2N\text{-}C_6F_4\text{-}O)_5$ (**6**) and $Cs_2Er(o\text{-}O_2N\text{-}C_6F_4\text{-}O)_5$ (**2**).
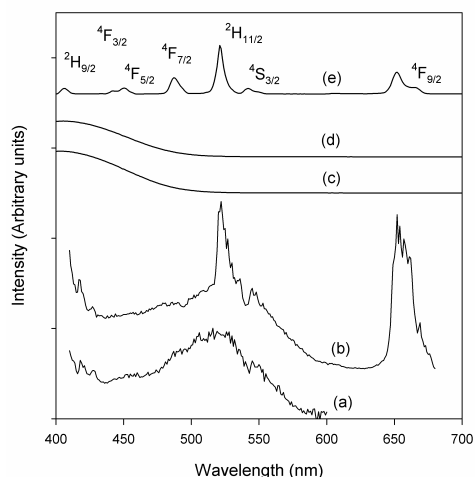
Figure 3. Photoluminescence excitation spectrum of (a) $Cs_2Yb(Et_2O)_{0.5}(o\text{-}O_2N\text{-}C_6F_4\text{-}O)_5$ (**6**) and (b) $Cs_2Er(o\text{-}O_2N\text{-}C_6F_4\text{-}O)_5$ (**2**). Also shown for comparison are the visible absorption data for $Cs_2Yb(Et_2O)_{0.5}(o\text{-}O_2N\text{-}C_6F_4\text{-}O)_5$ (**6**) in MeCN (spectrum c: λ_{max} 403 nm, ε 10400), $Cs_2Er(o\text{-}O_2N\text{-}C_6F_4\text{-}O)_5$ (**2**) in MeCN (spectrum d: λ_{max} 406 nm, ε 11000) and for a solution of $ErCl_3 \cdot 6H_2O$ in MeOH (spectrum e: λ_{max} 520 nm, ε 3.9).

Lifetime data were recorded at the peak of the photoluminescence spectra at a temperature of 300 K. For erbium this corresponded to the $^4I_{13/2} \rightarrow {}^4I_{15/2}$ transition (1545 nm) and for ytterbium the $^2F_{5/2} \rightarrow {}^2F_{7/2}$ transition (1032 nm). Lifetime data were fitted with either a one or two exponential decay model using a Marquardt-Levenberg algorithm to find the best fit.

The luminescence decay of the erbium complex **2** could be fitted by a single exponential function, giving a lifetime of 20.2 μs. As we have noted, it is very difficult to remove all traces of hydrogen-containing solvents from these materials. From recent work on deuterated $Cs[Er(HFA)_4]$ [7], it has been demonstrated that any C–H oscillators within 20 Å of an erbium ion can quench the lifetime to <100 μs, so the low levels of solvent detected in these samples would be sufficient to limit the lifetime to the observed value of 20.2 μs. Compared with the 1.8 μs lifetime observed for $Cs[Er(HFA)_4]$, where the hexafluoroacetylacetonate (HFA) ligands each contain a single C–H bond, there is a considerable extension in lifetime associated with exclusion of hydrogen from the environs of the erbium ion. The luminescence lifetime of the etherate **3** was 22.9 μs. Given that reproducibility of the lifetime measurements is of the order of ± 5%, there does not appear to be a significant difference in lifetime between the two samples.

The luminescence decay of the ytterbium complex **6** was best described using two lifetimes: 142 μs (92%) and 351 μs (8%), both of which greatly exceed the value of 21.6 μs observed for $Cs[Yb(HFA)_4]$. It has been previously noted by Faulkner that the luminescence in crystalline samples does not always undergo a simple exponential decay [3d], and that this may be due to surface effects. In the case of compound **6** the relative proximity of Yb^{3+} ions to residual solvent molecules could significantly affect their lifetimes.

Photoluminescence of the yttrium complex **4** was excited using wavelengths of 355 nm and 410 nm to investigate the ligand luminescence in the absence of an optically active ion. The luminescence spectra are shown in Figure 4. For the 355 nm excitation a peak at ~430 nm can be seen which extends towards 700 nm. At 410 nm excitation there is some evidence of the short wavelength peak being present, modified by the presence of a 435 nm high pass filter in the beam path to remove the pump laser, but the spectrum is dominated by a longer wavelength peak at *ca* 650 nm. Both of these emission bands overlap the main absorption bands of erbium in the visible region of the spectra and this probably accounts for the fast coupling observed between the ligand and the erbium ion. It can be seen that the longer wavelength emission extends to >800 nm which just brings it within the energy of the absorption into the $^2F_{5/2}$ level for ytterbium. This may therefore account for the ability of the ligand to act as a sensitizer for ytterbium. It is possible that the longer wavelength peak observed with 410 nm excitation is radiative recombination of the triplet state. A similar change in the ligand luminescence from singlet to triplet state as the excitation wavelength is increased was observed in aluminium tris(8-hydroxyquinolinate) [30].
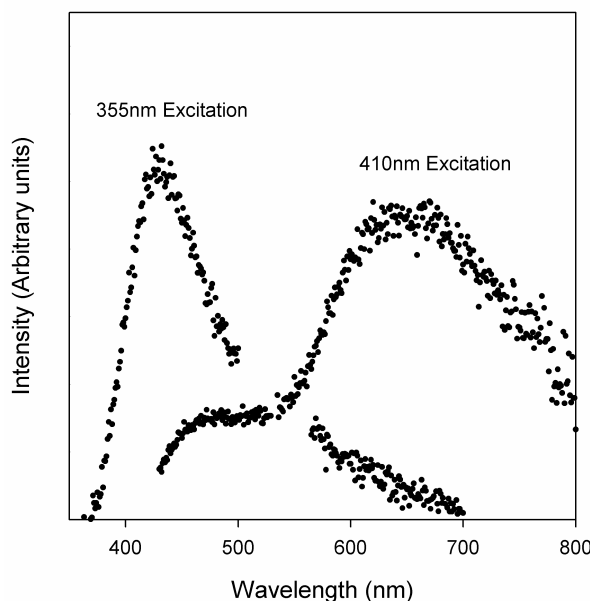
Figure 4. Photoluminescence spectra of $Cs_2Y(o\text{-}O_2NC_6F_4O)_5$ **4** at two excitation wavelengths.

4 Conclusions. We have structurally characterized the first examples of rare earth pentakis(3,4,5,6-tetrafluoro-2-nitrophenoxide) complexes and have shown that this ligand can form chelates with tripositive rare earth ions in a similar way to the non-fluorinated 2-nitrophenoxide. It can completely displace water from the coordination sphere of the rare earth, thus allowing synthesis to be performed in aqueous solution. The erbium and ytterbium complexes **2** and **6** luminesce in the infrared and have luminescence lifetimes far exceeding those of typical hydrogen-containing ligands.

The tetrafluoro-2-nitrophenoxide ligand absorbs blue and ultraviolet light quite strongly and shows a small antenna effect for photoexcitation of Er^{3+} and Yb^{3+} ions by visible light. Whereas the complexes are unsuitable for vacuum deposition, they are soluble in organic solvents and capable of being processed in solution.

Appendix A. Supplementary data

CCDC 627887, 642285, 627886 and 627885 contain the supplementary crystallographic data for **2**, **3**, **5** and **7** respectively. These data can be obtained free of charge via http://www.ccdc.cam.ac.uk/conts/retrieving.html or from the Cambridge Crystallographic Data Centre, 12 Union Road, Cambridge CB2 1EZ, UK; fax (+44) 1223-336-033; or email: deposit@ccdc.cam.ac.uk.

References

[1](a) J.-C. G. Bünzli, C. Piguet, Chem. Soc. Rev. 34 (2005) 1048;

(b) S. Comby, J.-C. G. Bünzli, Lanthanide Near-infrared Luminescence in Molecular Probes and Devices, Ch. 235 in Handbook on the Physics and Chemistry of Rare Earths, Vol. 37, Ed. K. A. Gschneidner, J.-C. G. Bünzli, V. K. Pecharsky, Elsevier, 2007.

[2](a) A. Beeby, S. Faulkner, D. Parker, J. A. G. Williams, J. Chem. Soc., Perkin Trans. 2 (2001) 1268;

(b) S. Faulkner, M.-C. Carrié, S. J. A. Pope, J. Squire, A. Beeby, P. G. Sammes, Dalton Trans. (2004) 1405;

(c) B. P. Burton-Pye, S. L. Heath, S. Faulkner, Dalton Trans. (2005) 146;

(d) S. J. A. Pope, B. P. Burton-Pye, R. Berridge, T. Khan, P. J. Skabara, S. Faulkner, Dalton Trans. (2006) 2907;

(e) H. Wang, G. Qian, M. Wang, J. Zhang, Y. Luo, J. Phys. Chem. B 108 (2004) 8084;

(f) S. Quici, M. Cavazzini, G. Marzanni, G. Accorsi, N. Armaroli, B. Ventura, F. Barigelletti, Inorg. Chem. 44 (2005) 529;

(g) R. Van Deun, P. Fias, P. Nockemann, A. Schepers, T. N. Parac-Vogt, K. Van Hecke, L. Van Meervelt, K. Binnemans, Inorg. Chem. 43 (2004) 8461;

(h) R. Van Deun, P. Fias, P. Nockemann, K. Van Hecke, L. Van Meervelt, K. Binnemans, Inorg. Chem. 45 (2006) 10416;

(i) S. Comby, D. Imbert, C. Vandevyver, J.-C. G. Bünzli, Chem. Eur. J., 13 (2007) 936.

[3] (a) N. M. Shavaleev, L. P. Moorcraft, S. J. A. Pope, Z. R. Bell, S. Faulkner, M. D. Ward, Chem. Eur. J. 9 (2003) 5283;

(b) S. J. A. Pope, B. J. Coe, S. Faulkner, E. V. Bichenkova, X. Yu, K. T. Douglas, J. Am. Chem. Soc. 126 (2004) 9490;

(c) F. Kennedy, N. M. Shavaleev, T. Koullourou, Z. R. Bell, J. C. Jeffery, S. Faulkner, M. D. Ward, Dalton Trans. (2007) 1492;

(d) T. K. Ronson, T. Lazarides, H. Adams, S. J. A. Pope, D. Sykes, S. Faulkner, S. J. Coles, M. B. Hursthouse, W. Clegg, R. W. Harrington, M. D. Ward, Chem. Eur. J. 12 (2006) 9299.

[4](a) Q. Zhong, H. Wang, G. Qian, Z. Wang, J. Zhang, J. Qiu, M. Wang, Inorg. Chem. 45 (2006) 4537;

(b) L. Song, Q. Wang, D. Tang, X. Liu, Z. Zhen, New. J. Chem. 31 (2007) 506.

[5] Y. Hasegawa, Y. Wada, S. Yanagida, J. Photochem. Photobiol C: Photochem. Rev. 5 (2004) 183.

[6] (a) Y. Hasegawa, Y. Kimura, K. Murakoshi, Y. Wada, J.-H. Kim, N. Nakashima, T. Yamanaka, S. Yanagida, J. Phys. Chem. 100 (1996) 10201;

(b) A. Beeby, I. M. Clarkson, R. S. Dickins, S. Faulkner, D. Parker, L. Royle, A. S. de Sousa, J. A. G. Williams, M. Woods, J. Chem. Soc., Perkin Trans. 2 (1999) 493;

(c) G. A. Hebbink, D. N. Reinhoudt, F. C. J. M. van Veggel, Eur. J. Org. Chem. (2001) 4101.

[7] R. H. C. Tan, M. Motevalli, I. Abrahams, P. B. Wyatt, W. P. Gillin, J. Phys. Chem. B 110 (2006) 24476.

[8] (a) Y. Hasegawa, T. Ohkubo, K. Sogabe, Y. Kawamura, Y. Wada, N. Nakashima, S. Yanagida, Angew. Chem. Int. Ed. 39 (2000) 357;

(b) R. Van Deun, P. Nockemann, C. Görller-Walrand, K. Binnemans, Chem. Phys. Lett. 397 (2004) 447;

(c) B. Chen, Y. Yang, F. Zapata, G. Qian, Y. Luo, J. Zhang, E. B. Lobkowsky, Inorg. Chem. 45 (2006) 8882.

[9] (a) G. Mancino, A. J. Ferguson, A. Beeby, N. J. Long, T. S. Jones, J. Am. Chem. Soc. 127 (2005) 524;

(b) A. P. Bassett, R. Van Deun, P. Nockemann, P. B. Glover, B. M. Kariuki, K. Van Hecke, L. Van Meervelt, Z. Pikramenou, Inorg. Chem. 44 (2005) 6140;

(c) P. B. Glover, A. P. Bassett, P. Nockemann, B. M. Kariuki, R. Van Deun, Z. Pikramenou, Chem. Eur. J. 13 (2007) 6308.

[10] F. Auzel, D. Meichenin, A. Mendorioz, R. Balda, J. Fernandez, J. Lumin. 72-74 (1997) 152.

[11] H. V. R. Dias, S. Singh, J. A. Flores, Inorg. Chem. 45 (2006) 8859.

[12] F. Babudri, G. M. Farinola, F. Naso, R. Ragni, Chem. Commun. (2007) 1003.

[13] F. Quochi, R. Orrù, F. Cordella, A. Mura, G. Bongiovanni, F. Artizzu, P. Deplano, M. L. Mercuri, L. Pilia, A. Serpe, J. Appl. Phys. 99 (2006) 053520.

[14] M. R. Bürgstein, M. T. Gamer, P. W. Roesky, J. Am. Chem. Soc. 126 (2004) 5213.

[15] J. M. Birchall, R. N. Haszeldine, J. Nikokavouras, E. S. Wilks, J. Chem. Soc. C (1971) 562.

[16] R. Hooft, *Collect: Data collection software*, Nonius BV, Delft, The Netherlands, 1998.

[17] Z. Otwinowski, W. Minor, Methods in Enzymology, Volume 276, Macromolecular Crystallography, part A, pp 307-326 (1997) C. W. Carter Jr., R. M. Sweet, Eds., Academic Press.

[18] S. Mackay, C.J. Gilmore, C. Edwards, M. Tremayne, N. Stewart, K. Shankland, *maXus solution and refinement software suite: maXus: a computer program for the solution and refinement of crystal structures from diffraction data*, University of Glasgow, Scotland, UK, Nonius BV, Delft, The Netherlands and MacScience Co. Ltd., Yokohama, Japan, 1998.

[19] (a) R. H. Blessing, Acta Cryst. A51 (1995) 33;

(b) R.H. Blessing, J. Appl. Cryst. 30 (1997) 421.

[20] Enraf-Nonius *CAD-4/PC* Software, Version 1.5c, Enraf-Nonius, Delft, The Netherlands, 1994.

[21] A. C. T. North, D. C. Phillips, F. S. Mathews, Acta Crystallogr., Sect. A 42 (1968) 351.

[22] K. Harms, S. Wocadlo, *XCAD4 – CAD4 Data Reduction*, University of Marburg, Marburg, Germany, 1995.

[23] P. T. Beurskens, G. Beurskens, W. P. Bosman, R. de Gelder, S. Garcia-Granda, R. O. Gould, R. Israel, J. M. M. Smits, *DIRDIF-99 Program System*, Crystallography Laboratory, University of Nijmegen, The Netherlands, 1999.

[24] G. M. Sheldrick, *SHELX Suite of Programs for Crystal Structure Analysis (Release 97-2)*, University of Göttingen, Germany, 1998.

[25] L. J. Farrugia, J. Appl. Cryst. 30 (1997) 565.

[26] A. L. Spek, *PLATON, A Multipurpose Crystallographic Tool*, Utrecht University, Utrecht, The Netherlands, 1998.

[27] L. J. Farrugia, J. Appl. Cryst. 32 (1999) 837.

[28] (a) J. M. Harrowfield, L. Weimin, B. W. Skelton, A. H. White, Aust. J. Chem. 47 (1994) 321;

(b) J. M. Harrowfield, L. Weimin, B. W. Skelton, A. H. White, Aust. J. Chem. 47 (1994) 339;

(c) K.-Z. Tang, J. Zhang, Y. Tang, W.-S. Liu, M.-Y. Tan, Y.-X. Sun, Inorg. Chim. Acta 359 (2006) 1207;

(d) M. I. Saleh, E. Kusrini, R. Adnan, B. Saad, B. M. Yamin, H. K. Fun, J. Mol. Struct. 837 (2007) 169.

[29] H. Plenio, Chem. Rev. 97 (1997) 3363.

[30] R.J. Curry, W.P. Gillin, J. Appl. Phys. 88 (2000) 781.